Acta Cryst. (1975). B31, 2759

The Superstructure of the Intermediate Pyrrhotite. I. Partially Disordered Distribution of Metal Vacancy in the 6*C* Type, $Fe_{11}S_{12}$

BY KICHIRO KOTO, NOBUO MORIMOTO AND ATSUO GYOBU*

Institute of Scientific and Industrial Research, Osaka University, Suita, Osaka 565, Japan

(*Received* 25 *January* 1975; *accepted* 28 *April* 1975)

The intermediate pyrrhotite with the compositional range from Fe_9S_{10} (the 5*C* type) to $Fe_{11}S_{12}$ (6*C*) has a complex superstructure of the NiAs type with various non-integral *c* periods from five to six times as long as a sub-period. The 6*C* pyrrhotite is monoclinic (pseudo-orthorhombic) with $a=6{\cdot}8950$ (2), $b=11{\cdot}9536$ (4), $c=34{\cdot}518$ (2) Å and $\beta=90{\cdot}00$ (5)°. The diffraction aspect is *F-/d*. The distribution of Fe vacancy has been determined with the aid of a Patterson function whose coefficients were obtained by extrapolating the averages of unitary intensities for various groups of superstructure reflexions to $(\sin\theta)/\lambda=0$. The superstructure is statistical and a filled layer of Fe atoms alternates with two consecutive defective layers along the *c* axis. The sequence of Fe layers along the *c* axis is represented by: $F\,D_AD_AF\,D_BD_BF\,D_CD_CF\,D_DD_DF\,D_AD_AF\ldots$, where *F* represents a filled layer and $D_A, D_B, \ldots$, defective layers in which $A, B, \ldots$ sites are each occupied by one half of an Fe atom. The statistical structure can be interpreted as forming a domain texture.

Introduction

Five types of pyrrhotite with stoichiometric compositions of Fe_7S_8 (the 4*C* type), Fe_9S_{10} (5*C*), $Fe_{10}S_{11}$ (11*C*), $Fe_{11}S_{12}$ (6*C*) and FeS (2*C*), have been found to occur naturally (Morimoto, Nakazawa, Nishiguchi & Tokonami, 1970). All these types except the 2*C* have a superstructure of the NiAs-type due to partial defects of Fe atoms. A recent study on natural specimens, however, indicates that the intermediate pyrrhotites have the compositional range from Fe_9S_{10} to $Fe_{11}S_{12}$ with various long *c* periods, non-integral multiples of the fundamental *C* length (Morimoto, Gyobu, Tsukuma & Koto, 1975).

The structure of the 2*C* pyrrhotite (troilite) has been determined by Bertaut (1956) and refined by Evans (1970). The structure of the 4*C* pyrrhotite has been determined by Bertaut (1953) as having an Fe filled layer alternating with a defective layer parallel to (001). Tokonami, Nishiguchi & Morimoto (1972) carried out the refinement and confirmed the structure of Bertaut. Van Landuyt & Amelinckx (1972) studied the 4*C* pyrrhotite by an electron microscope and observed various kinds of defect such as anti-phase boundaries, stacking faults and twin boundaries, which were predicted from the structure model. The structure of the trigonal phase (Fe_7S_8) quenched from 500°C was studied by Fleet (1971).

Corlett (1968) proposed that the structure of the 5*C* pyrrhotite is obtained by adding two filled layers to the Fe_7S_8 cell and every fifth two-iron-layer unit consists of two filled layers. Nakazawa & Morimoto (1971) mentioned the possibility of Fe vacancies occurring in every third iron layer in the structure of the 6*C* pyrrhotite. However their proposed structures have not been confirmed on the basis of the intensity data. A recent study of the pyrrhotite by the lattice-image technique with high-resolution electron microscopy has provided some aspects of the structure (Nakazawa, Morimoto & Watanabe, 1974; Morimoto, Nakazawa & Watanabe, 1974; Pierce & Buseck, 1974).

The origin of superstructure reflexions of the intermediate pyrrhotite can be attributed, as in the 4*C* pyrrhotite, first, to an ordered distribution of Fe vacancies and secondly, to a displacement of S and Fe atoms from their positions in the fundamental NiAs-type structure. The former controls the main scheme of the structure. In the present investigation, the distribution of vacancies for Fe atoms in the superstructure of the 6*C* pyrrhotite has been determined with the aid of a Patterson function whose coefficients are the unitary intensities which were obtained by a statistical treatment of the X-ray data.

Experimental

A single crystal of the 6*C* pyrrhotite was obtained by examining many crystals from Chigusa, Makimine mine, Japan, by X-rays. It shows almost orthorhombic symmetry but a slight lowering of symmetry to monoclinic was observed in the intensity distribution. The supercell has $\mathbf{a}=2\mathbf{A}_1$, $\mathbf{b}=2\mathbf{A}_1+4\mathbf{A}_2$ and $\mathbf{c}=6\mathbf{C}$ where $\mathbf{A}_1$, $\mathbf{A}_2$ and $\mathbf{C}$ represent the hexagonal NiAs-type subcell vectors (Fig. 1). The subcell dimensions are metrically almost hexagonal. However, orthorhombic deformation was observed on the back-reflexion Weissenberg films at about $2\theta=130°$. The cell dimensions were obtained by the least-squares method with data on back-reflexion films around two axes using Si as internal

---

* Present address: Niihama Technical College, 7-1 Yakumo, Niihama 792, Japan.

standard and Fe $K\alpha_1$ and $K\alpha_2$ radiation (1·93597 and 1·93991 Å, respectively). $a=6\cdot8950$ (2), $b=11\cdot9536$ (4), $c=34\cdot518$ (2) Å and $\beta=90\cdot00$ (5)°. Possible space group is *Fd* or *F*2/*d* from the diffraction aspect. A unit cell contains eight chemical formulae of $\mathrm{Fe_{11}S_{12}}$ with eight vacant sites for Fe atoms (Morimoto *et al.*, 1975).

Intensity data up to $(\sin\theta)/\lambda=0\cdot60$ were collected on a Rigaku four-circle diffractometer by the ω–2θ scan technique, with Mo $K\alpha$ radiation monochromatized by pyrolytic graphite. A single crystal $0\cdot003\times0\cdot002\times0\cdot01$ cm was used. The 1255 independent reflexions were measured and the usual data reduction was applied. No absorption or extinction corrections were made. 650 reflexions had intensities greater than $2\sigma(I)$ and were regarded as observed, where $\sigma(I)$ represents the standard deviation calculated from counting statistics.

Classification of superstructure reflexions

In the 6*C* pyrrhotite structure, S atoms are arranged in hexagonal closest packing and Fe atoms are distributed in the octahedral interstices of the S atoms. In the centrosymmetric space group *F*2/*d*, the coordinates of the equivalent positions are as follows (Tokonami *et al.*, 1972):

$$(0,0,0;\ \tfrac{1}{2},\tfrac{1}{2},0;\ \tfrac{1}{2},0,\tfrac{1}{2};\ 0,\tfrac{1}{2},\tfrac{1}{2})\\ +x,y,z;\ \tfrac{1}{4}-x,y,\tfrac{1}{4}-z;\ \bar{x},\bar{y},\bar{z};\ \tfrac{1}{4}+x,\bar{y},\tfrac{1}{4}+z\ .$$

The ideal coordinates of the atoms are reasonably assumed to be $\frac{3}{8},\frac{1}{24},(4m-1)/24$ and $\frac{3}{8},\frac{5}{24},(4m+1)/24$ for S, where $m=0,1,2$, and $\frac{1}{8},\frac{1}{8},n/12$ for Fe, where $n=2,3,\cdots,7$. All Fe atoms are in the general position which has 16 equivalent sites. Because a unit cell contains eight Fe vacancies, Fe atoms must be statistically distributed in six crystallographically different positions in this space group. Therefore the completely ordered structure must have the space group *Fd* in which each general position has eight equivalent sites.

Attempts to determine the structure based on complete ordering of Fe vacancies have been unsuccessful, with discrepancies between the observed and calculated structure factors of particular superstructure reflexions, indicating that the distribution of the Fe atoms is statistical. The structure has been determined with the following procedure starting from the assumption of the non-centrosymmetric space group *Fd*.

The coordinates of equivalent positions in *Fd* are given as follows:

$$(0,0,0;\ \tfrac{1}{2},\tfrac{1}{2},0;\ \tfrac{1}{2},0,\tfrac{1}{2};\ 0,\tfrac{1}{2},\tfrac{1}{2})+x,y,z;\ \tfrac{1}{4}+x,\bar{y},\tfrac{1}{4}+z.$$

The geometrical structure factor is expressed as

$$G=4\exp 2\pi i(hx+ky+lz)\{1+\exp \pi i(h-8ky+l)/2\}$$

for *h*, *k* and *l* all even or all odd. It becomes zero for other indices. The coordinates of atoms without displacement from their positions in the fundamental NiAs-type structure are reasonably assumed to be $\frac{3}{8},\frac{1}{24},(4m-1)/24$ and $\frac{3}{8},\frac{5}{24},(4m+1)/24$ for S, where $m=0,1,\cdots,5$, and $\frac{1}{8},\frac{1}{8},n/12$ for Fe, where $n=0,1,2,\cdots,11$. Let the occupancy probability of Fe vacancy be p_n where $0\le p_n\le 1$ and the atomic scattering factors for S and Fe, f_{S} and f_{Fe}, respectively. The structure factor is expressed as

$$\begin{aligned}F_{hkl}&=f_{\mathrm{S}}G_{\mathrm{S}}+f_{\mathrm{Fe}}\exp\{\pi i(h+k)/4\}[1+\exp\{\pi i(h-k\\&\quad+l)/2\}]\sum_{n=0}^{11}(1-p_n)\exp(\pi i l n/6)\\&=f_{\mathrm{S}}G_{\mathrm{S}}+f_{\mathrm{Fe}}G_{\mathrm{Fe}}-4f_{\mathrm{Fe}}\exp\{\pi i(h+k)/4\}\\&\quad\times[1+\exp\{\pi i(h-k+l)/2\}]\sum_{n=0}^{11}p_n\exp(\pi i l n/6)\end{aligned}$$

where

$$\begin{aligned}G_{\mathrm{S}}&=4\exp\{\pi i(3h/4+k/12)\}[1+\exp\{\pi i(3h-k\\&\quad+3l)/6\}]\sum_{m=0}^{5}\exp\{\pi i l(4m-1)/12\}+4\exp\{\pi i(3h/4\\&\quad+5k/12)\}[1+\exp\{\pi i(3h-5k+3l)/6\}]\end{aligned}$$

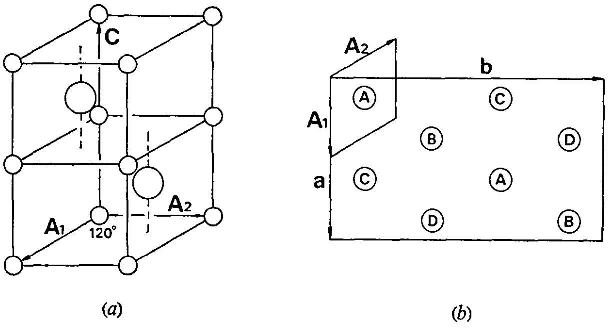

(*a*) (*b*)

Fig. 1. (*a*) The fundamental NiAs-type structure with the hexagonal cell edges of A and C Large circles represent S atoms and small circles, Fe atoms. (*b*) Subcell and supercell of the 6*C* pyrrhotite. *A*, *B*, *C* and *D* represent the sites of four crystallographically different Fe rows along the *c* axis.

Table 1. *The h, k and l dependence of* φ *and* $|\varphi|^2$

M and *N* are integers.

h, *k* and *l*	all even				all odd	
$h+k$	$4M$		$4M+2$		$4M$	$4M+2$
l	$4N$	$4N+2$	$4N$	$4N+2$	$2N+1$	$2N+1$
φ	$2\times(-1)^M$	0	0	$2i\times(-1)^M$	$(-1)^M\times\{1-i(-1)^N\}$	$i(-1)^M\times\{1+i(-1)^N\}$
$\lvert\varphi\rvert^2$	4	0	0	4	2	2

$$\times \sum_{m=0}^{5} \exp\{\pi i l(4m+1)/12\}$$

and

$$G_{\mathrm{Fe}} = 4\exp\{\pi i(h+k)/4\}[1+\exp\{\pi i(h-k+l)/2\}] \times \sum_{n=0}^{11} \exp(\pi i l n/6)\,.$$

Here $f_S G_S + f_{\mathrm{Fe}} G_{\mathrm{Fe}}$ is the structure factor of the fundamental NiAs-type structure without Fe vacancy, and is different from zero when h, k and l are all even, $h+k=4M$ and $l=6N$ with the exception of $l=12N$ for $00l$, where M and N are integers. The Fe vacancy is required to have a negative atomic scattering factor $-f_{\mathrm{Fe}}$ and its geometrical structure factor is expressed as

$$G_V = 4\varphi \times \sum_{n=0}^{11} p_n \exp(\pi i l n/6)$$

where

$$\varphi = \exp\{\pi i(h+k)/4\}\ [1+\exp\{\pi i(h-k+l)/2\}]\,.$$

The h, k and l dependence of φ is shown in Table 1.

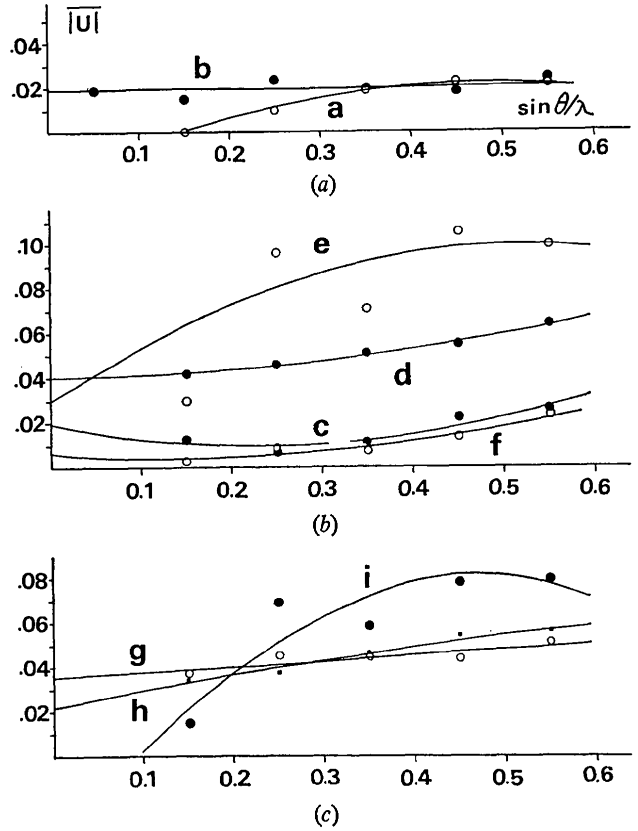

Fig. 2. Averages of unitary intensity are plotted against $(\sin\theta)/\lambda$ for nine groups of superstructure reflexions. (*a*) h and k both even and $h+k=4M$; (*b*) h and k both even and $h+k=4M+2$; (*c*) h and k both odd. Symbols of groups, $a, b, \ldots, i$, are identical with those in Table 2. The curves were obtained by the least-squares method.

The geometrical intensity due to vacancies, $|G_V|^2$, is calculated for the reflexions for 11 different groups as follows. When h, k and l are all even and $h+k=4M$, then

$$\begin{aligned} |G_V|^2 &= 64\Big|\sum_{n=0}^{11} p_n\Big|^2 && \text{for } l=12N \\ &= 0 && \text{for } l=12N\pm 2 \\ &= 64\Big|\sum_{n=0}^{11} p_n \exp(2\pi i n/3)\Big|^2 && \text{for } l=12N\pm 4 \\ &= 0 && \text{for } l=12N\pm 6. \end{aligned}$$

When h, k and l are all even and $h+k=4M+2$, then

$$\begin{aligned} |G_V|^2 &= 0 && \text{for } l=12N \\ &= 64\Big|\sum_{n=0}^{11} p_n \exp(\pi i n/3)\Big|^2 && \text{for } l=12N\pm 2 \\ &= 0 && \text{for } l=12N\pm 4 \\ &= 64\Big|\sum_{n=0}^{11} p_n \cos \pi n\Big|^2 && \text{for } l=12N\pm 6. \end{aligned}$$

When h, k and l are all odd, then

$$\begin{aligned} |G_V|^2 &= 32\Big|\sum_{n=0}^{11} p_n \exp(\pi i n/6)\Big|^2 && \text{for } l=12N\pm 1 \\ &= 32\Big|\sum_{n=0}^{11} p_n \exp(\pi i n/2)\Big|^2 && \text{for } l=12N\pm 3 \\ &= 32\Big|\sum_{n=0}^{11} p_n \exp(5\pi i n/6)\Big|^2 && \text{for } l=12N\pm 5\,, \end{aligned}$$

where M and N are integers. The result indicates that the geometrical intensity of the superstructure reflexions due to the vacancy distribution is the same for all reflexions in the same group and the seven groups can have non-zero values. However, the reflexions of the other four groups with a zero value for $|G_V|^2$ actually show some non-zero intensity because of the displacement of atoms. Since the first and fourth groups belong to the fundamental NiAs-type reflexions, the other nine groups are for the superstructure reflexions. Because the asymmetric unit contains a vacancy, $\sum_{n=0}^{11} p_n = 1$ and therefore $|G_V|^2 = 64$ for the first group.

Unitary intensity

A Wilson (1942) plot cannot be applied to the case of superstructure in general. In order to obtain the absolute scale factor, the substructure or the average structure with **A** and **C** was first determined. The 93 substructure reflexions corresponding to the fundamental NiAs-type structure were used for this purpose.

Although Fe atoms may be arranged in order at crystallographically different sites in the superstructure, they are superposed in the average structure. Space group $P6_3/mmc$ was assumed for the average structure, as for the NiAs-type, where S atoms are at $(\frac{1}{3},\frac{2}{3},\frac{1}{4})$ and $(\frac{2}{3},\frac{1}{3},\frac{3}{4})$ and Fe atoms, at (0,0,0) and $(0,0,\frac{1}{2})$ [Fig. 1(*a*)]. Two sites for Fe atoms in the average structure are equivalent. The population of Fe sites should be 0·917 according to the chemical formula of $Fe_{11}S_{12}$. One scale factor and two isotropic temperature factors for S and Fe atoms were refined by the least-squares method. The *R* value is 0·072 for the 93 reflexions. The temperature factors are 1·03 (21) and 1·93 (14) Å^2 for S and Fe atoms, respectively. Because these values are only apparent ones on account of the superposition of atoms which may be displaced from their positions in the fundamental NiAs-type structure, they are not appropriate for the calculation of the unitary intensity given by $|U|^2=|\sum_{j=1}^{N} n_jG_j|^2$; here $n_j=f_j/\sum_{j=1}^{N} f_j$. Isotropic temperature factors for the 4*C* pyrrhotite (Tokonami *et al.*, 1972), the structure of which is analogous to that of the 6*C* pyrrhotite in that the superstructure is based on the ordering of Fe vacancies, were assigned. Their average temperature factors are 0·69 and 0·99 for S and Fe atoms, respectively. The unitary intensities of superstructure reflexions of the 6*C* pyrrhotite were calculated with these values and the scale factor for the average structure.

Averages of unitary intensity of superstructure reflexions

The superstructure reflexions were classified into nine groups. Besides the six groups due to both vacancy distribution and displacement of atoms, three other groups were considered, the intensities of which are due only to displacement of atoms. The averages of the unitary intensity are plotted against $(\sin\theta)/\lambda$ for each group of superstructure reflexions (Fig. 2).

Although the unitary intensity due to the vacancy distribution is constant for each group of superstructure reflexions, the intensity due to the displacement of atoms depends on both $(\sin\theta)/\lambda$ and the feature of the intensity distribution of the substructure reflexions. The unitary intensity due to the vacancy distribution can be obtained by extrapolating the intensity averages for each group of superstructure reflexions to $(\sin\theta)/\lambda=0$. The non-zero intercepts at $(\sin\theta)/\lambda=0$, represent the unitary intensity due to the vacancy distribution of Fe atoms. The values of intercepts at $(\sin\theta)/\lambda=0$, $|U_0|$, are in Table 2. All the curves except those for two groups are almost smooth with a gentle slope. Two

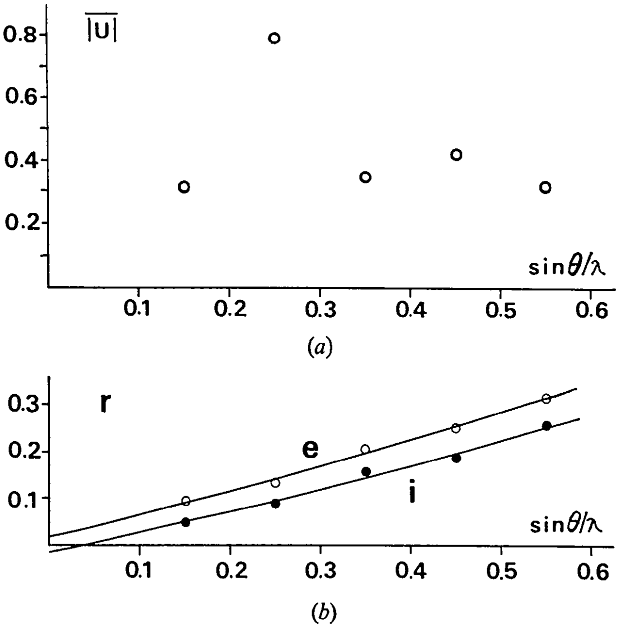

Fig. 3. (*a*) Averages of unitary intensity, $\overline{|U|}$, of the substructure reflexions are plotted against $(\sin\theta)/\lambda$. Deviation from a smooth curve is observed. (*b*) The ratio to the averages of substructure reflexions, *r*, for the two groups of superstructure reflexions whose averages are not on smooth curves (Fig. 2).

Table 2. *Intercepts, $|U_0|$, of the unitary intensity curves of the superstructure reflexions at $(\sin\theta)/\lambda=0$ for the 6C pyrrhotite as determined by the least-squares method*

M and *N* are integers. Superstructure reflexions of (*a*), (*c*) and (*e*), are due to the displacement of atoms. They are expected to be zero at $(\sin\theta)/\lambda=0$ theoretically and were omitted in the calculation of the Patterson function.

Index			$\lvert U_0\rvert$ obs.	$\lvert U_0\rvert$ calc.†
h and *k*		both even		
(*a*)	$h+k=4M$	and $l=12N\pm2$	$-0·023\pm0·001$	0·0
(*b*)		and $l=12N\pm4$	$0·018\pm0·003$	0·027
(*c*)	$h+k=4M+2$	and $l=12N$	$0·020\pm0·003$	0·0
(*d*)		and $l=12N\pm2$	$0·040\pm0·001$	0·047
(*e*)		and $l=12N\pm4$	$0·014\pm0·009$*	0·0
(*f*)		and $l=12N\pm6$	$0·007\pm0·002$	0·0
h and *k*		both odd		
(*g*)		and $l=12N\pm1$	$0·035\pm0·002$	0·037
(*h*)		and $l=12N\pm3$	$0·022\pm0·002$	0·027
(*i*)		and $l=12N\pm5$	$-0·017\pm0·009$*	0·010

* This value is the ratio to the unitary intensity of substructure reflexions [see the text and Fig. 3(*b*)]. A negative value of *i* is regarded as zero in the calculation of the Patterson function.

† Calculated value of the unitary intensity based on the structure obtained (Fig. 4).

groups with h and k both even, $h+k=4M+2$ and $l=12N\pm4$, and with h and k both odd, and $l=12N\pm5$ [(*e*) and (*i*) in Fig. 2, respectively], do not show a smooth curve. Because their values rapidly become larger with increasing $(\sin\theta)/\lambda$, the origin of their intensity is mainly due to the displacement of S and/or Fe atoms in the fundamental structure. If the contribution from the displacement of atoms to the total intensity is significant, the intensity of the superstructure reflexions should depend on the feature of the intensity distribution of the substructure reflexions. The ratio of the intensity of the superstructure reflexions to that of their substructure reflexions is expected to become a smooth curve against $(\sin\theta)/\lambda$ (Toman & Frueh, 1971). This is the case for the above two groups (Fig. 3).

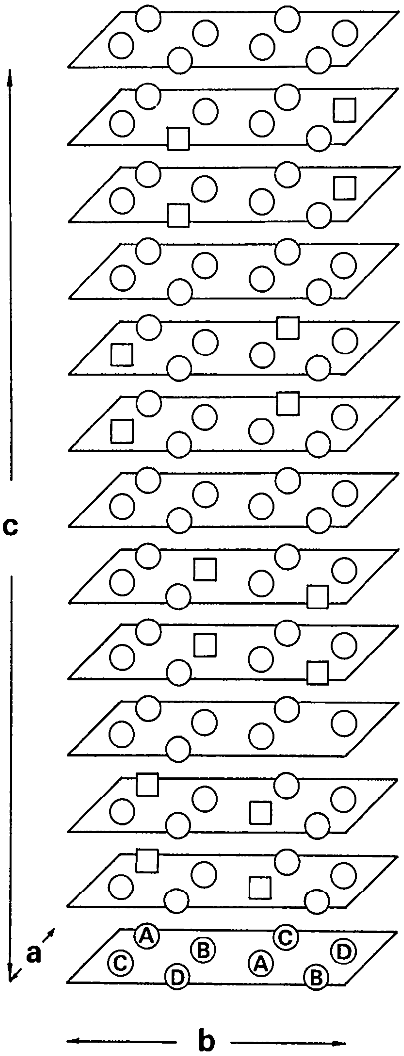

Fig. 4. The superstructure of the 6*C* pyrrhotite $Fe_{11}S_{12}$. Only Fe atoms which are at the octahedral site of S atoms are shown. Squares represent occupation of one half of an Fe atom.

Distribution of the Fe vacancies

In order to determine the arrangement of the Fe vacancies, the Patterson function was calculated by using the unitary intensity, $|U_0|^2$, as coefficient. The non-zero values of five groups [(*b*), (*d*), (*f*), (*g*) and (*h*) in Table 2] were used for the calculation. The unitary intensity due to vacancy distribution for one of the two groups of the fundamental NiAs-type reflexions (h, k and l all even, $h+k=4M$ and $l=12N$), was given theoretically as

$$|U_V|^2=\{f_{Fe}G_V/(96f_S+88f_{Fe})\}^2=0{\cdot}054^2$$

where $G_V=8$, $f_S=16$ and $f_{Fe}=26$ for $(\sin\theta)/\lambda=0$ and used for the calculation.

Since this Patterson function shows only the vectors between Fe vacancies in the superstructure, the distribution of Fe vacancy could be determined from this function. The coordinates of the vacancies are $\frac{1}{8},\frac{1}{8},\frac{1}{12}$ and $\frac{1}{8},\frac{1}{8},\frac{1}{6}$ and $p=0{\cdot}5$ for both sites and therefore, the vacancy distribution is centrosymmetric. The calculated value of the unitary intensity based on this vacancy distribution is compared with the observed value (Table 2).

The displacement of S and Fe atoms from the fundamental structure has been determined by the Fourier syntheses and by the least-squares method. The details of the result will be published elsewhere.

Description

In the structure of the 6*C* pyrrhotite, Fe atoms are in the octahedral interstices of the hexagonal close-packed S atoms as in other pyrrhotite structures. The vacancy distribution in the 12 Fe layers along the *c* axis is statistical but a filled layer of Fe atoms always alternates with two consecutive defective layers along the *c* axis (Fig. 4). In every defective layer, one of the four crystallographically different sites for Fe atoms is occupied by one half of an Fe atom and the other three, each by an Fe atom. In the two successive layers sandwiched between filled layers, the site with the same *x* and *y* coordinates is vacant for Fe. The sequence of Fe layers along the *c* axis is, therefore, represented by: $F\ D_AD_AF\ D_BD_BF\ D_CD_CF\ D_DD_DF\ D_AD_AF\ D_BD_BF\ D_CD_CF\ D_DD_DF\ldots$, where F represents a filled layer and $D_A, D_B,\ldots$, defective layers in which each of the $A, B,\ldots$ sites is occupied by one half an Fe atom. The x and y coordinates of A, B, C and D sites are $(0,0;\frac{1}{2},\frac{1}{2})+\frac{1}{8},\frac{1}{8};\ \frac{3}{8},\frac{3}{8};\ \frac{5}{8},\frac{3}{8}$ and $\frac{7}{8},\frac{3}{8}$, respectively.

It seems very unlikely that two defective sites are in succession in an Fe row along the *c* axis because this arrangement makes the distance between the vacancies too close. Even in the structure of the 4*C* pyrrhotite, which is the most Fe deficient, no consecutive defective layers of Fe are observed. Therefore the statistical structure of the 6*C* pyrrhotite obtained by the X-ray analysis can be interpreted as forming a domain texture of units where every defective layer is followed by a filled layer. Two most probable models for the 6C pyrrhotite are:

(*a*) $F\ F\ D'_A F\ F\ D'_B F\ F\ D'_C F\ F\ D'_D F\ F\ D'_A F$
$F\ D'_B F\ F\ D'_C F\ F\ D'_D \ldots$
$+ F\ D'_A F\ F\ D'_B F\ F\ D'_C F\ F\ D'_D F\ F\ D'_A F\ F$
$D'_B F\ F\ D'_C F\ F\ D'_D F \ldots$

and

(*b*) $F\ F\ D'_A F\ D'_B F\ F\ F\ D'_C F\ D'_D F\ F\ F\ D'_A F$
$D'_B F\ F\ F\ D'_C F\ D'_D F \ldots$
$+ F\ D'_A F\ F\ F\ D'_B F\ D'_C F\ F\ F\ D'_D F\ D'_A F\ F$
$F\ D'_B F\ D'_C F\ F\ F\ D'_D \ldots$

where $D'_A, D'_B, \ldots$ represent the defective layers with an Fe vacancy at $A, B, \ldots$. In the (*a*) structure, the defective layers distribute as far apart as possible. To explain the statistical structure, the relative relation of the domains must be given by a definite out-of-step vector of $\mathbf{c}/12 = \mathbf{C}/2$. In the (*b*) structure a pair of defective layers, between which is one filled layer, is essential. The sequence unit of the five Fe layers, *FDFDF*, is part of the structure of the 4C pyrrhotite which is represented as $F\ D'_A F\ D'_B F\ D'_C F\ D'_D F\ D'_A F\ D'_B F\ D'_C F\ D'_D F \ldots$. The relative relation of the domains must be given by the n glide plane at $b/4$.

The structure of the 6C pyrrhotite is compared with that of the 4C pyrrhotite (Fig. 5). In the structure of the 4C pyrrhotite, the vacancies are completely ordered. However, in the structure of the 6C pyrrhotite, the vacancies are partially disordered. In both structures, two kinds of misalignment with vectors such as $(\mathbf{a}+\mathbf{b})/4$ and $(\mathbf{a}-\mathbf{b})/4$ take place alternately every $\mathbf{c}/4$ with respect to the Fe vacancy. Non-integral-type superstructures of the intermediate pyrrhotite with the compositional range from Fe_9S_{10} to $Fe_{11}S_{12}$ are also explained by the same misalignments and will be studied in part II.

The authors wish to express their thanks to Professor J. Kakinoki, Faculty of Science, Osaka City University, for helpful comments and discussions. They also thank Dr M. Tokonami of this Institute and Mr M. Kitamura, Faculty of Science, Tohoku University, for their discussions.

All computations in the present investigation were carried out at the Computation Centres of Osaka University and University of Tokyo, using the UNICS System (Sakurai, 1967).

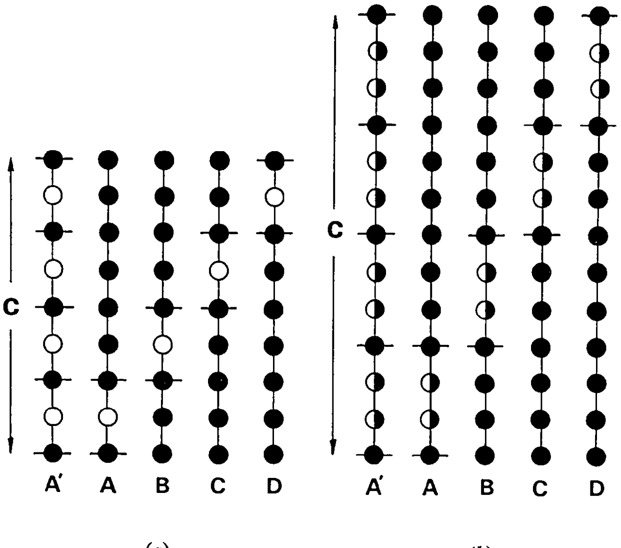

Fig. 5. Distribution of Fe vacancies in four different rows (*A*, *B*, *C* and *D*) are shown for (*a*) the 4C pyrrhotite Fe_7S_8 and (*b*) the 6C pyrrhotite $Fe_{11}S_{12}$. The *A* prime row represents a hypothetical Fe row at *A* before misalignment takes place.

References

Bertaut, E. F. (1953). *Acta Cryst.* **6**, 557–561.
Bertaut, E. F. (1956). *Bull. Soc. Fr. Minér. Crist.* **79**, 276–292.
Corlett, M. (1968). *Z. Kristallogr.* **126**, 124–134.
Evans, H. T. Jr (1970). *Science*, **167**, 621–623.
Fleet, M. E. (1971). *Acta Cryst.* B**27**, 1864–1867.
Morimoto, N., Gyobu, A., Tsukuma, K. & Koto, K. (1975). *Amer. Min.* **77**, 234–260.
Morimoto, N., Nakazawa, H., Nishiguchi, K. & Tokonami, M. (1970). *Science*, **168**, 964–966.
Morimoto, N., Nakazawa, H. & Watanabe, E. (1974). *Proc. Japan Acad.* **50**, 756–759.
Nakazawa, H. & Morimoto, N. (1971). *Mat. Res. Bull.* **6**, 345–358.
Nakazawa, H., Morimoto, N. & Watanabe, E. (1974). *Proc. 8th Int. Congr. Electron Microsc.* **1**, 478–499.
Pierce, L. & Buseck, P. R. (1974). *Science*, **186**, 1209–1212.
Sakurai, T. (1967). UNICS System, Cryst. Soc. Japan.
Tokonami, M., Nishiguchi, K. & Morimoto, N. (1972). *Amer. Min.* **57**, 1066–1080.
Toman, K. & Frueh, A. J. (1971). *Acta Cryst.* B**27**, 2182–2186.
Van Landuyt, J. & Amelinckx, S. (1972). *Mat. Res. Bull.* **7**, 71–79.
Wilson, A. J. C. (1942). *Nature, Lond.* **150**, 151–152.